

1  
2 DR JAMES FREDERICK MARKWORTH (Orcid ID : 0000-0002-5348-1464)

3  
4  
5 Article type : Original Paper

6  
7  
8 **Metabolipidomic Profiling Reveals an Age-Related Deficiency of Skeletal Muscle Proresolving Mediators**  
9 **that Contributes to Maladaptive Tissue Remodeling**

10  
11 **Running title:** Role of Specialized Proresolving Mediators in Muscle Aging

12  
13 James F. Markworth<sup>1</sup>, Lemuel A. Brown<sup>1</sup>, Eunice Lim<sup>1</sup>, Jesus A. Castor-Macias<sup>2</sup>, Jacqueline Larouche<sup>2</sup>, Peter  
14 C. D. Macpherson<sup>1</sup>, Carol Davis<sup>1</sup>, Carlos A. Aguilar<sup>2</sup>, Krishna Rao Maddipati<sup>3</sup>, Susan V. Brooks<sup>1,2</sup>

15  
16 <sup>1</sup>Department of Molecular & Integrative Physiology, University of Michigan, Ann Arbor, Michigan.

17 <sup>2</sup>Department of Biomedical Engineering, University of Michigan, Ann Arbor, Michigan.

18 <sup>3</sup>Department of Pathology, Lipidomics Core Facility, Wayne State University, Detroit, Michigan.

19  
20 Susan V. Brooks, PhD

21 Christin Carter-Su Collegiate Professor of Physiology

22 Professor of Biomedical Engineering

23 Professor of Molecular & Integrative Physiology

24 University of Michigan

25 2029 BSRB

This is the author manuscript accepted for publication and has undergone full peer review but has not been through the copyediting, typesetting, pagination and proofreading process, which may lead to differences between this version and the [Version of Record](#). Please cite this article as [doi: 10.1111/ACEL.13393](https://doi.org/10.1111/ACEL.13393)

This article is protected by copyright. All rights reserved

26 109 Zina Pitcher Pl.

27 Ann Arbor, MI 48109-2002

28 (734) 936-2147

29 [svbrooks@umich.edu](mailto:svbrooks@umich.edu)

30  
31  
32  
33  
34 **Summary:**

35 Specialized proresolving mediators actively limit inflammation and support tissue regeneration, but their  
36 role in age-related muscle dysfunction has not been explored. We profiled the mediator lipidome of aging  
37 muscle via liquid chromatography-tandem mass spectrometry and tested whether treatment with the  
38 proresolving mediator resolvin D1 (RvD1) could rejuvenate the regenerative ability of aged muscle. Aged mice  
39 displayed chronic muscle inflammation and this was associated with a basal deficiency of proresolving  
40 mediators 8-oxo-RvD1, resolvin E3, and maresin 1, as well as many antiinflammatory cytochrome P450-  
41 derived lipid epoxides. Following muscle injury, young and aged mice produced similar amounts of most  
42 proinflammatory eicosanoid metabolites of cyclooxygenase (e.g. prostaglandin E<sub>2</sub>) and 12-lipoxygenase (e.g.  
43 12-hydroxy-eicosatetraenoic acid), but aged mice produced less markers of proresolving mediators including  
44 the lipoxins (15-hydroxy-eicosatetraenoic acid), D-resolvins/protectins (17-hydroxy-docosahexaenoic acid), E-  
45 resolvins (18-hydroxy-eicosapentaenoic acid), and maresins (14-hydroxy-docosahexaenoic acid). Similar  
46 absences of downstream proresolving mediators including lipoxin A<sub>4</sub>, resolvin D6, protectin D1/DX, and  
47 maresin 1 in aged muscle were associated with greater inflammation, impaired myofiber regeneration, and  
48 delayed recovery of strength. Daily intraperitoneal injection of RvD1 had minimal impact on intramuscular  
49 leukocyte infiltration and myofiber regeneration, but suppressed inflammatory cytokine expression, limited  
50 fibrosis, and improved recovery of muscle function. We conclude that aging results in deficient local  
51 biosynthesis of specialized proresolving mediators in muscle and that immunoresolvents may be attractive  
52 novel therapeutics for the treatment of muscular injuries and associated pain in the elderly, due to positive  
53 effects on recovery of muscle function without the negative side effects on tissue regeneration of non-steroidal  
54 anti-inflammatory drugs.

## Introduction:

Aging results in a progressive decline in skeletal muscle mass and function that contributes to frailty, loss of mobility, and increased mortality in the elderly (Faulkner, Larkin, Claflin, & Brooks, 2007). Aged muscles are also more susceptible to damage and have a reduced ability to regenerate successfully if injured (Blau, Cosgrove, & Ho, 2015). Potential sources of this dysfunction include a chronic accumulation of macrophages (M $\Phi$ ) within muscle in advanced age (Wang, Wehling-Henricks, Samengo, & Tidball, 2015), as well as dysregulated acute myeloid cell responses to muscle injury (Sloboda, Brown, & Brooks, 2018). On this basis, targeting the immune system has shown promise to rejuvenate the regenerative capacity of aged muscle and limit age-associated muscle wasting (Tidball, Flores, Welc, Wehling-Henricks, & Ochi, 2021).

The immune response to muscle injury begins with rapid infiltration of neutrophils, followed by blood monocyte-derived M $\Phi$  that initially exhibit a proinflammatory phagocytic phenotype, but later act to support muscle regeneration (Arnold et al., 2007). In general, resolution of the acute inflammatory response is actively controlled by endogenous specialized proresolving mediators that inhibit further recruitment of neutrophils, while stimulating regenerative M $\Phi$  functions (Chiang & Serhan, 2020). Docosahexaenoic acid (DHA) is the precursor to proresolving mediators including the D-series resolvins (Serhan et al., 2002), protectins (Mukherjee, Marcheselli, Serhan, & Bazan, 2004), and maresins (Serhan et al., 2009). In endogenous routes of their biosynthesis, 15-lipoxygenase (15-LOX) initially oxygenates DHA to form 17(S)-hydroxy-DHA (17-HDoHE), a key intermediate metabolite in production of both the D-series resolvins (e.g. RvD1) and protectins (e.g. PD1) (Hong, Gronert, Devchand, Moussignac, & Serhan, 2003). Alternatively, the 12-LOX pathway produces 14(S)-hydroxy-DHA (14-HDoHE), a key pathway marker of the maresins (e.g. MaR1) (Serhan et al., 2009). Additional important members of this family of metabolites include the arachidonic acid (ARA) derived

This article is protected by copyright. All rights reserved

lipoxins (e.g. LXA<sub>4</sub>) (Serhan, Hamberg, & Samuelsson, 1984) and eicosapentaenoic acid (EPA) derived E-series resolvins (e.g. RvE1) that are generated via the initial formation of 15(S)-hydroxy-eicosatetraenoic acid (15-HETE) and 18(R)-hydroxy-eicosapentaenoic acid (18-HEPE), respectively (Arita et al., 2005; Serhan et al., 1984).

Specialized proresolving mediators are produced in response to muscle injury (Giannakis et al., 2019; Markworth et al., 2020; Sansbury et al., 2020; M. J. Zhang et al., 2016) or physiological stress (Gangemi et al., 2003; Markworth et al., 2013; Vella et al., 2019; Zheng, Pena Calderin, Hill, Bhatnagar, & Hellmann, 2019) implicating a role for these metabolites in muscle remodelling (Markworth, Maddipati, & Cameron-Smith, 2016). Current approaches to clinical management of soft tissue injuries focus predominantly on blocking cyclooxygenase (COX) mediated production of proinflammatory prostaglandins with non-steroidal anti-inflammatory drugs (NSAIDs). However NSAIDs also interfere with biosynthesis of proresolving mediators (Markworth et al., 2013), which can delay timely resolution of inflammation (Schwab, Chiang, Arita, & Serhan, 2007), with potential deleterious effects on muscle repair (Markworth et al., 2016). In contrast to NSAIDs, resolution agonists can stimulate muscle repair and may thus offer an attractive alternative to classical anti-inflammatory approaches (Giannakis et al., 2019; Markworth et al., 2020; McArthur et al., 2020; Sansbury et al., 2020; M. J. Zhang et al., 2016).

Aging is associated with a deficiency of specialized proresolving mediators in peritoneal fluid (Arnardottir, Dalli, Colas, Shinohara, & Serhan, 2014), heart (Halade, Kain, Black, Prabhu, & Ingle, 2016), central nervous system (Krashia et al., 2019), and lungs (Rymut et al., 2020). Indeed, mice lacking the key resolution sensor, lipoxin A<sub>4</sub>/formyl peptide receptor 2 (ALX/FPR2), develop a premature aging phenotype (Tourki et al., 2020). Conversely, treatment of aged mice with RvD1, an endogenous ALX/FPR2 ligand, can stimulate resolution in models of peritonitis (Arnardottir et al., 2014) and ischemia-perfusion induced lung injury (Rymut et al., 2020). RvD1 was also recently shown to be of therapeutic benefit in a rat model of Parkinson's disease by modulating neuroinflammation (Krashia et al., 2019). The endogenous role and potential therapeutic applicability of specialized proresolving mediators in the context of skeletal muscle aging has however not been examined.

In the current study we investigated the effect of aging on the basal mediator lipidome of skeletal muscle as well as intramuscular lipid mediator production in response to sterile injury. Furthermore, we tested whether RvD1 treatment could limit inflammation and stimulate muscle regeneration in aged mice.

## Results:

### Age-Associated Loss of Muscle Mass and Strength

Aged mice (26-28 mo) had similar body weights, but lower tibialis anterior (TA) muscle mass than young mice (4-6 mo) (Figure 1A). Maximal *in-situ* nerve-stimulated TA isometric force ( $P_o$ ) was lower in aged mice and this deficit persisted after accounting for their smaller muscle size (specific  $P_o$ ,  $sP_o$ ) (Figure 1B). TA muscles from aged mice contained similar total numbers of myofibers, but had a substantial reduction in mean myofiber cross-sectional area (CSA) (Figure 1D). Aging also resulted in a loss of type IIa and IIx fibers, an increase in IIb fibers, and a reduction in mean CSA for all type II fibers (Figure 1E). These data show that these mice developed a robust sarcopenic phenotype in advanced age.

### Chronic Low-grade Inflammation of Aged Muscle is Associated with a Lack of Anti-Inflammatory and Pro-Resolving Lipid Mediators

In order to investigate the mechanisms that may contribute to age-associated muscle atrophy and weakness, we first performed targeted liquid chromatography-tandem mass spectrometry-based (LC-MS/MS) based profiling of uninjured TA muscle homogenates from young and aged mice. Intramuscular concentrations of all detected metabolites are presented in Supplemental Tables 1A-E. Unsupervised principle component analysis (PCA) score plots revealed a clear clustering of samples by age (Figure 2A). Corresponding loading plots show key representative metabolites from each major enzymatic pathway that contributed to this response

(Figure 2B). Overall the lipid mediator profile of young muscle was characterized by an abundance of polyunsaturated fatty acid (PUFA) metabolites, many of which are common products of the 5-LOX, 15-LOX, and CYP pathways. Of the 98 total lipid mediator species detected in muscle homogenates, 35 were present at significantly lower concentration (1.5-fold,  $p < 0.05$ ) in samples from aged mice, while none were significantly enriched (Figure 2C). A complete list of fold changes, p-values, and associated false discovery rates for each analyte is shown in Supplemental Table 2A.

Cumulative metabolites of the COX-1 and 2 pathways encompassing the thromboxanes and prostaglandins were similarly abundant in young and aged muscle (Figure 2D, Supplemental Table 1A) with no individual COX metabolites differing between young and aged mice (Supplemental Table 2A). In contrast, pooled products of the 5-LOX and 15-LOX pathways were substantially lower in aged mice (Figure 2D, Supplemental Table 1B). Most notably, this included 15-HETE, the primary 15-LOX derived metabolites of ARA which is a key pathway marker of the lipoxins (Supplemental Tables 1B and 2A). On the other hand, 17-HDoHE, the primary 15-LOX metabolite of DHA and key D-series resolvins biosynthetic marker did not differ between young and aged muscle at baseline. Nevertheless, 5-LOX metabolites of both ARA [5-hydroxy-eicosatetraenoic acid (5-HETE)] and DHA [7-hydroxy-docosaheptaenoic acid (7-HDoHE)], additional pathway markers of the lipoxins and D-resolvins respectively, were lower in aged vs young muscle (Supplemental Tables 1B and 2A). Finally, the overall activity of the CYP pathway, which primarily generates antiinflammatory epoxide metabolites such as the epoxy-eicosatrienoic acids (EpETrEs), but also produces the key E-series resolvins pathway marker 18-HEPE, was markedly lower in aged muscle (Figure 2D, Supplemental Table 1C). Indeed, 18-HEPE was ~30% lower in aged vs young muscle, although this did not reach statistical significance ( $p = 0.14$ ) (Supplemental Table 2A). Downstream di- and tri-hydroxy-PUFA metabolites, which are produced endogenously by the sequential action of two or more different LOX and/or CYP isoforms, were generally present at very low concentrations in muscle and were often below the limits of detection (Supplemental Table 1D). Nevertheless, bioactive specialized proresolving mediators (abbreviated as SPM in Figure 2 and 3) including LXA<sub>4</sub>, resolvins D6 (RvD6), MaR1, and MaR1<sub>n-3</sub> DPA were detected in all samples, while resolvins E3 (RvE3) and 8-oxo-RvD1 were detected only in young muscle (Figure 2C, Supplemental Table 1D). There was an overall basal deficiency of pooled specialized proresolving mediators in aged mice (Figure 2D), predominantly attributable to significantly lower concentrations of MaR1 (Supplemental Table 1D, Supplemental Table 2A).

The deregulated mediator lipidome of aged muscle was accompanied by increased muscle mRNA expression of cytokines and immune cell markers, as well as greater intramuscular numbers of neutrophils, total MΦ, M2-like MΦ, and to a lesser extent M1-like MΦ ( $p = 0.09$ ) (Figure 2H-K), although the ratio of M2:M1-like

MΦ did not differ between young and aged mice (2.17 vs. 1.64,  $p=0.34$ ). This chronic accumulation of MΦ in aged muscle was further confirmed by flow cytometry (Supplemental Figure 1). Inflammation of aged muscle was associated with increased centrally nucleated fibers supporting ongoing myofiber degeneration/regeneration (Figure 2L). Representative images illustrating intramuscular myeloid cell populations are shown in Figure 2M. Overall, the data show that chronic inflammation of aging muscle is characterized by a basal deficiency of proresolving lipid mediators.

### **Aged Mice Mount a Deficient Specialized Proresolving Lipid Mediator Response to Muscle Injury**

We next assessed the effect of aging on local lipid mediator biosynthesis following muscle injury induced by intramuscular injection of barium chloride ( $\text{BaCl}_2$ ). There was a minor shift in global muscle lipid mediator profile at day 1 post-injury (Figure 3A), due predominantly to a rapid increase in likely non-enzymatic PUFA metabolites (Figure 3B, Supplemental Table 1E). This was followed by a marked shift in muscle lipid mediator profile at day 3 post-injury attributable to increased concentrations of many major products of the COX, LOX, and CYP pathways (Figure 3A-B, Supplemental Tables 1A-D).

When compared to young mice, aged mice mounted an overall deregulated lipid mediator response as evidenced by less separation of clusters of samples obtained at distinct time-points within respective PCA score plots (Figure 3A). Analysis of intramuscular lipid mediators pooled over major biosynthetic pathways by two-way ANOVA revealed that aged and young mice produced similar cumulative amounts of COX, 12-LOX, and CYP products following injury (age  $\times$  time effects of  $p=0.33$ ,  $p=0.74$ ,  $p=0.27$  respectively) (Figure 3B). In contrast, aged mice showed diminished local production of cumulative metabolites of the 5-, 8-, and 15-LOX pathways, as well as a marked deficiency in pooled detected downstream bioactive specialized proresolving mediators (age  $\times$  time  $p=0.018$ ,  $p=0.048$ ,  $p=0.013$ ,  $p=0.036$  respectively) (Figure 3B).

A heat map summarizing the temporal shifts in key individual lipid mediator species is shown in Figure 3C. There were age-related deficiencies in biosynthesis of LXA<sub>4</sub>, RvD6, protectin D1 (PD1), protectin DX (PDX), and MaR1 (Supplemental Table 1D and 2B-D). Key pathway markers of the lipoxins (15-HETE), D-resolvins (17-HDoHE), E-resolvins (18-HEPE), and maresins (14-HDoHE) were also all produced to a significantly lesser extent in aged muscle following injury (Supplemental Table 1B and Supplemental Table 2C-D). On the other hand, young and aged mice displayed largely equivalent production of many proinflammatory eicosanoid metabolites of the COX pathway [e.g. thromboxane B<sub>2</sub> (TXB<sub>2</sub>), prostaglandin E<sub>2</sub> (PGE<sub>2</sub>), and prostaglandin F<sub>2 $\alpha$</sub>  (PGF<sub>2 $\alpha$</sub> )] and 12-LOX pathway [e.g. 12-hydroxy-eicosatetraenoic acid (12-HETE)] (Supplemental Table 1A and 2B-D). Notable exceptions were prostaglandin D<sub>2</sub> (PGD<sub>2</sub>) and 13,14-dihydro-15-keto PGD<sub>2</sub>, the cyclopentenone prostaglandins J<sub>2</sub> (PGJ<sub>2</sub>) and 15-deoxy- $\Delta$ 12,14- PGJ<sub>2</sub>, as well as prostaglandin I<sub>2</sub> (PGI<sub>2</sub> or prostacyclin), measured as its degradation product 6-keto-prostaglandin F<sub>1 $\alpha$</sub>  (6kPGF<sub>1 $\alpha$</sub> ), all of which

This article is protected by copyright. All rights reserved

were significantly lacking in aged muscle following injury. The blunted proresolving mediator response in aged muscle resulted in a relative overabundance of pooled eicosanoids following injury (Figure 3D). Kinetic data for major individual prostaglandins, detected specialized proresolving mediators, and related LOX and CYP derived pathway markers is shown in Supplemental Figure 2.

With the exception of an initial transient increase in muscle mass at day 1 post-injury in aged mice, temporal shifts in the masses of the TA muscles used for lipidomic profiling were similar between young and aged mice (Figure 3E). Volcano plots summarizing the overall differences between aged and young muscle mediator lipidomes for all detected analytes at each time-point are shown in Figure 3F and Supplemental Table 2B-D. These findings demonstrate that aging results in a marked imbalance in local biosynthesis of inflammatory and resolving lipid mediators following muscle damage.

### **Resolvin D1 Treatment Suppresses Intramuscular Inflammatory Cytokines, but Does Not Limit Excessive Leukocyte Infiltration of Aged Muscle**

Since aging was associated with impaired proresolving mediator biosynthesis in response to muscle injury, we aimed to investigate whether treatment of aged mice with exogenous proresolving molecules might limit muscle inflammation and improve regeneration. We chose to test RvD1 due to its well-established dose-response pharmacokinetics (Sun et al., 2007), stimulatory effects on muscle regeneration in young mice (Markworth et al., 2020; Sansbury et al., 2020), and ability to protect aged mice from ischemia-reperfusion induced lung injury (Rymut et al., 2020). Finally, 17-HDoHE, the primary 15-LOX-derived precursor to RvD1 was detected in muscle, markedly increased following injury, but significantly impaired in aged mice.

We first confirmed that RvD1 treatment stimulated phagocytosis by bone marrow-derived M $\Phi$  in vitro and showed that M $\Phi$  from aged mice maintained the intrinsic ability to respond effectively to RvD1 (Supplemental Figure 3). We then treated aged mice with RvD1 at a dose of 100 ng/day administered by intraperitoneal injection. This route and dose was based on many prior studies (e.g Markworth et al., 2020; Sansbury et al., 2020). We did not measure the its pharmacokinetics, but RvD1 is well-known to rapidly appear in peripheral circulation following intraperitoneal injection (Krashia et al., 2019).

At day 1 post-injury, there was a large increase for both age groups in intramuscular neutrophils (Ly6G<sup>+</sup> cells) and M $\Phi$  (CD68<sup>+</sup> cells) that was followed by a subsequent decline in Ly6G<sup>+</sup> cells and progressive M $\Phi$  recruitment peaking at day 3 (Figure 4A-4B). When compared to young mice, aged mice initially showed relatively greater recruitment of Ly6G<sup>+</sup> cells at 1-day post-injury, but more significant clearance by day 3 (Figure 4C-D), with a relatively greater intramuscular M $\Phi$  presence at both day 1 and day 3 post-injury (Figure 4C-D). Treatment of aged mice with RvD1 did not influence myeloid cell numbers in muscle (Figure 4C-D).



To confirm the surprising finding that despite a markedly deficient local biosynthetic response for specific proresolving mediators in aged mice, the rate of clearance of neutrophils from injured muscle was accelerated, we repeated these experiments for analysis of the whole intramuscular single cell population by flow cytometry. At day 3 post-injury ~8% of intramuscular leukocytes (CD45<sup>+</sup> cells) were Ly6G<sup>+</sup> in young mice, compared with only ~2% in aged mice (Figure 4E). This was accompanied by a parallel increase in the proportion of MΦ (CD64<sup>+</sup> cells) in aged muscle. Treatment of aged mice with RvD1 did not influence the proportion of CD45<sup>+</sup> cells that were either Ly6G<sup>+</sup> or CD64<sup>+</sup> (Figure 4E). RvD1 treatment did however reduce muscle mRNA expression of cytokines within injured muscle (Figure 4F). Thus, RvD1 may still influence the inflammatory profile of intramuscular leukocytes despite not impacting their number.

### **Defective Myofiber Regeneration in Aged Mice is not Influenced by RvD1**

Many small myofibers with characteristic centrally located nuclei and robust expression of embryonic myosin heavy chain (eMHC) appeared by day 5 post-injury in both young and aged mice (Figure 5A). When compared to young mice, regenerating muscle cross-sections from aged mice contained fewer newly formed myofibers (as assessed by the combination of eMHC expression and associated centrally located myonuclei) (Figure 5B). In addition to a lack of fibers undergoing regeneration in aged mice, the myofibers that were regenerating were smaller in size (Figure 5C-D). RvD1 treatment did not influence regenerating fiber number or size (Figure 5A-C).

When compared to young mice, aged muscles tended to have more total MΦ at day 5 post-injury ( $p=0.09$ ), and this was especially true for M2-like MΦ (CD68<sup>+</sup>CD163<sup>+</sup> cells) (Figure 5E). Treatment of aged mice with RvD1 did not impact intramuscular MΦ (Figure 5F). Muscle satellite cells (MuSC) increased markedly at day 5 post-injury, aged mice showed lower numbers of MuSCs than young mice, and this was reduced even further by RvD1 treatment (Figure 5G-H). Thus, RvD1 treatment had a marked impact on the MuSC response to muscle damage but this did not translate to a clear positive or negative impact on myofiber regeneration.

### **RvD1 Limits Maladaptive Remodeling of Aged Muscle and Improves Recovery of Muscle Function**

When expressed relative to age-matched uninjured muscles (Figure 1), aged mice had greater deficits than young mice at 14 days' post-injury for  $P_0$  and much of this difference persisted after accounting for the smaller regenerating muscle size in aged mice ( $sP_0$ ), while treatment with RvD1 tended to improve this  $sP_0$  deficit ( $p=0.06$ ) (Figure 6A). To investigate the basis for the functional improvement, we performed hematoxylin and eosin staining and found that compared to young mice, regenerating muscles from untreated aged mice had a greatly expanded interstitial space between their smaller regenerating myofibers (Figure 6B).

271 Aged TA muscle cross-sections were overall smaller in size than young mice and this was mainly due to a  
272 reduction in muscle fiber (actin<sup>+</sup>) area, while the amount of extracellular matrix (actin<sup>-</sup> area) was similar to  
273 young muscle (Figure 6C). Because of this, regenerating aged muscles were comprised of a greater proportion  
274 of non-contractile tissue, indicative of poorer muscle quality and reflected in the sP<sub>o</sub> deficit. When compared to  
275 aged mice receiving vehicle treatment, RvD1 did not influence overall muscle size or total myofiber (actin<sup>+</sup>)  
276 area, but did reduce the amount of intramuscular non-contractile (actin<sup>-</sup>) tissue (Figure 6C). Consequently, the  
277 relative proportion of muscle which was compromised of functional myofibers was increased in aged mice  
278 treated with RvD1 when compared to untreated aged mice.

279 Neither age nor RvD1 treatment had a significant impact on the fiber type composition of regenerating  
280 muscles (Figure 6D) and both young and aged TA muscles were predominantly composed of regenerating  
281 myofibers at day 14 post-injury (Figure 6E). When compared to young mice, aged muscles contained fewer  
282 regenerating myofibers which were on average smaller in size, but this was not influenced by RvD1 treatment.  
283 Aged muscles also still contained many more intramuscular MΦ than young mice even at 2-weeks following  
284 muscle damage and treatment of aged mice with RvD1 did not influence this response (Supplemental Figure 4).

## 289 Discussion:

290 We examined the effect of aging on the local lipid mediator response to muscle injury and tested  
291 whether systemic RvD1 treatment limits inflammation and improves muscle regeneration in aged mice. Aged  
292 mice produced similar amounts of proinflammatory prostaglandins (e.g. PGE<sub>2</sub>) as young mice following injury,  
293 but displayed deficient intramuscular markers of specialized proresolving mediator biosynthesis, as well as a  
294 lack of several downstream lipoxins, resolvins, protectins, and maresins. This deregulated lipid mediator  
295 response was associated with excessive inflammation, deficient myofiber regeneration, increased fibrosis, and  
296 delayed functional recovery. Treatment of aged mice with RvD1 limited inflammatory cytokine expression, but  
297 did not impact myeloid cell recruitment or myofiber regeneration. Nevertheless, RvD1 limited maladaptive  
298 tissue remodeling resulting in improved recovery of muscle specific force. These findings reveal an age-  
299 associated imbalance of intramuscular inflammatory and resolving lipid mediators and support  
300 immunoresolvents as an attractive alternative for the clinical management of muscle injuries and associated pain

in the elderly, due to positive effects on recovery of strength without negative side effects of NSAIDs on muscle regeneration.

Consistent with recent reports, we found a chronic age-associated increase in muscle neutrophils (Kawanishi & Machida, 2021; Li et al., 2020; Sloboda et al., 2018) and M2-like M $\Phi$  (Cui et al., 2019; Jensen et al., 2020; Reidy et al., 2019; Sorensen et al., 2019; Wang et al., 2015). Aged mice also mounted a heightened acute inflammatory response to muscle injury, which is also consistent with prior studies (Blanc et al., 2020; Patsalos et al., 2018; Rahman, Angus, Stokes, Karpowicz, & Krause, 2020; Sloboda et al., 2018). LC-MS/MS based profiling revealed that this greater inflammation was associated with a deficiency in local biosynthesis of key pathway markers in the biosynthesis of the lipoxins (15-HETE), E-resolvins (18-HEPE), D-resolvins/protectins (17-HDoHE), and maresins (14-HDoHE). While di- and tri-hydroxylated PUFA metabolites were only sporadically detectable within muscle homogenates, several downstream bioactive specialized proresolving mediators including LXA<sub>4</sub>, RvD6, PD1, PDX, and MaR1 were also relatively lacking in aged muscle during regeneration.

Systemic treatment of aged mice with RvD1 has previously shown promise limiting leukocyte-induced lung injury (Rymut et al., 2020) and modulating neuroinflammation in a rat model of Parkinson's disease (Krashia et al., 2019). Furthermore, we and other groups recently showed that RvD1 treatment improved regenerative outcomes following muscle injury in young mice (Markworth et al., 2020; Sansbury et al., 2020). In the current study, treatment with RvD1 suppressed both pro and antiinflammatory cytokines in muscle of aged mice, but in contrast to our prior study in young mice, did not reduce early M $\Phi$  infiltration (Markworth et al., 2020). Other inflammation-related genes (e.g. TNF $\alpha$ , IL-6) that were markedly suppressed post-injury in young mice treated with RvD1 (Markworth et al., 2020), also only trended towards suppression in aged muscle here. Thus, RvD1 was unable to fully overcome heightened muscle myeloid cell infiltration in aged mice. This may relate to the increased inflammation-related gene expression in aged muscle even before injury. Therefore, future studies should examine whether longer-term immunoresolvent treatments may reduce chronic basal inflammation of aged muscle. Furthermore, a single immunoresolvent class may be insufficient for the overall resolution of inflammation following muscle injury, especially in aged mice which were deficient in markers of all major proresolving mediators. Therefore, therapeutic administration of different specialized proresolving mediators and/or combinatorial treatments may have additional therapeutic effects on age-related muscle dysfunction.

The 12-LOX pathway is classically known for producing the proinflammatory eicosanoid 12-HETE. However, the maresin family of specialized proresolving mediators are also formed via the 12-LOX pathway, by the initial conversion of DHA to 14-HDoHE (Serhan et al., 2009). Both 12-HETE and 14-HDoHE increased

333 in response to muscle injury in the current study and while the 14-HDoHE response was markedly blunted in  
334 aged compared with young mice, 12-HETE was not impacted by aging. How two distinct metabolic products of  
335 the same enzymatic pathway can be differently modulated in aging muscle remains unclear, but several  
336 plausible mechanisms exist. Firstly, the deficient 14-HDoHE response might originate from a deficiency in  
337 DHA, rather than defects in 12-LOX activity. Secondly, multiple 12-LOX isoforms exist, which differ in their  
338 substrate specificity, enzyme kinetics, and cell type expression profiles and only specific 12-LOX isoforms may  
339 be deregulated in aged muscle. Finally, production of specialized proresolving mediators involves multiple  
340 steps, often via transcellular biosynthetic routes involving two or more enzymes. Therefore, the lack of maresins  
341 in aged muscle might also result from 12-LOX independent mechanisms entirely, although our 14-HDoHE data  
342 would argue against this conclusion.

343 We also observed a marked deficit in aged muscle prior to injury in many epoxide metabolites derived  
344 from the less well explored CYP pathway which possess anti-inflammatory actions (Christmas, 2015). A recent  
345 study showed that PUFA epoxides also stimulate the resolution of inflammation and could thus be classed as  
346 proresolving mediators themselves (Gilroy et al., 2016). The CYP pathway also contributes to endogenous  
347 biosynthesis of the E-series resolvins by producing the key intermediate 18-HEPE (Arita et al., 2005). Indeed,  
348 we found 18-HEPE in abundance within injured muscle of young mice but markedly deficient in aged mice.  
349 Therefore, metabolites of the LOX and CYP pathways are likely to act in unison. While we focused our  
350 intervention on a LOX-derived resolvin, our data suggest that targeting the CYP pathway may be an additional  
351 novel strategy to combat basal age-associated muscle inflammation and related dysfunction.

352 The ability of RvD1 to limit neutrophil infiltration is well-described for certain experimental models of  
353 acute inflammation (Sun et al., 2007), but we have been unable to demonstrate this with sterile skeletal muscle  
354 injury (Markworth et al., 2020). The benefit of RvD1 on revascularization of ischemic skeletal muscle was  
355 recently found to be independent of effects on neutrophil infiltration (Sansbury et al., 2020). Therefore, the  
356 suppressive effects of RvD1 on neutrophil recruitment may depend on the nature of the inflammatory insult and  
357 the site of inflammation. A second defining action of specialized proresolving mediators is accelerating a return  
358 to a non-inflamed state by stimulating neutrophil clearance. Indeed, we previously found that RvD1 treatment  
359 reduced intramuscular neutrophil numbers by day 3 following muscle injury in young mice despite not limiting  
360 their initial appearance (Markworth et al., 2020). To our surprise, we found here that aged mice actually cleared  
361 these cells more rapidly than young mice and RvD1 treatment did not further accelerate the response.  
362 Neutrophils can inflict secondary muscle damage and limiting their influx is generally considered to be  
363 protective from muscle injury. Thus, the observation that aged muscle displayed both more rapid clearance of  
364 neutrophils and defective myofiber regeneration was surprising. Neutrophils do play an important role in

muscular adaptations under certain conditions however and as such future studies are needed to better clarify the role of these cells in aging muscle (Lockhart & Brooks, 2008).

Consistent with recent reports, we found that aged mice displayed marked defects in regenerating myofiber number and size (Blanc et al., 2020; Patsalos et al., 2018; Rahman et al., 2020; C. Zhang et al., 2020), but RvD1 treatment had minimal impact on this response. Aging is also well-established to limit recovery of muscle function following injury, due at least in part to an accumulation of fibrotic tissue during muscle regeneration (Rahman et al., 2020; C. Zhang et al., 2020). Indeed, we found that aged mice showed marked deficits in recovery of strength due to both reduced ability of aged muscle to recover its pre-injury size as well as maladaptive tissue remodeling that further impaired relative contractile function. Although treatment of aged mice with RvD1 did not impact any cellular indices of regenerating myofiber number/size or fiber type it did improve recovery of specific muscle force due to reduced accumulation of fibrotic tissue. Collectively, these data show that while RvD1 treatment appears unable to rescue age-related defects in myofiber regeneration, it nonetheless limited maladaptive tissue remodeling and thus improved the quality of the regenerated muscle resulting in improved contractile function.

Our findings are in contrast to the beneficial effects of RvD1 treatment on regenerating muscle fiber size observed previously in young mice with this same dosing regimen (Markworth et al., 2020), and recent reports that local intramuscular injection of a distinct but related proresolving mediator, resolvin D2 (RvD2), could also improve recovery of overall muscle size and strength (Giannakis et al., 2019). Additionally, RvD1 treatment stimulated revascularization of ischemic muscle in young mice (Sansbury et al., 2020). Consistent with our results are recent reports that systemic RvD1 treatment limited fibrosis of other tissues such as the heart (Hiram et al., 2020). Mice lacking the RvD1 receptor in all cell types (*Alx/Fpr2<sup>-/-</sup>* mice) or specifically in myeloid cells (*hALX/FPR2<sup>MKO</sup>* mice) both display increased muscle fibrosis following hind-limb ischemia (Sansbury et al., 2020). Thus, the age-associated deficiency of endogenous ALX/FPR2 ligands (e.g. LXA<sub>4</sub>) during muscle regeneration and protective effect of exogenous RvD1 treatment (an ALX/FPR2 ligand) on maladaptive muscle remodeling identified in the current study are most likely mediated via intramuscular myeloid cells.

In conclusion, aging leads to a local deficiency of intramuscular proresolving lipid mediator biosynthesis that is associated with chronic muscle inflammation, heightened acute myeloid cell responses to injury, and poor regenerative outcomes. Short term systemic treatment with RvD1 reduced local expression of inflammatory mediators and limited maladaptive tissue remodeling following muscle injury, but was unable to fully overcome age-associated defects in myofiber regeneration. Given their emerging important roles in stimulating tissue regeneration, other proresolving mediators such as the E-resolvins, protectins, and maresins,

396 which were also deficient in aged muscle, may contribute to age-related muscle dysfunction and warrant further  
397 investigation.

398  
399  
400  
401  
402  
403  
404  
405  
406  
407  
408  
409  
410  
411  
412  
413  
414  
415  
416  
417  
Author Manuscript

418 **Experimental Procedures:**

419 *Animals:* Aged female mice were obtained from the National Institute of Aging (NIA) at 20-22 mo,  
420 housed for ~6 months, and used for experiments between 26-28 mo. Adult (4-6 mo) female C57BL/6 mice were

obtained from Charles River Laboratories and served as young adult controls. All mice were housed under specific pathogen free conditions with ad-libitum access to food and water.

**Muscle Injury:** Mice were anesthetized with 2% isoflurane and received bilateral intramuscular injection of the tibialis anterior (TA) muscle with 50  $\mu$ L per limb of 1.2% BaCl<sub>2</sub> in sterile saline to induce myofiber injury. Mice were returned to their home cage to recover and monitored until ambulatory with free access to food and water.

**Immunoresolvent Treatment:** RvD1 was purchased from Cayman Chemicals (10012554). Aged mice were randomized to receive daily 100  $\mu$ L intraperitoneal (IP) injections of either 100 ng of RvD1 or vehicle control (0.1% ethanol) with the first dose given during ~5 min prior to muscle injury. Mice were allowed to recover for up to two-weeks with daily IP injection of 100 ng of RvD1 or vehicle control.

**M $\Phi$  phagocytosis:** To confirm the established bioactivity of RvD1 on myeloid cells we performed in-vitro phagocytosis assays using pHrodo Green *E. Coli* Bio Particles (Invitrogen, P35366) with bone-marrow derived macrophage (BMM) cultures isolated from young (4-6 mo) and aged (26-28 mo) host mice.

**Histology:** Cross-sections (10  $\mu$ m) were cut from the muscle mid-belly in a cryostat at -20°C and adhered to SuperFrost Plus slides. Sections were air dried and then stained with hematoxylin and eosin (H & E). Slides for immune cell staining were fixed in acetone at -20°C and then air dried. Satellite cell staining slides were fixed in 4% paraformaldehyde (PFA), quenched with hydrogen peroxide, and antigen retrieval performed. Unfixed tissue sections were used for muscle fiber type staining. Prepared slides were blocked in 10% normal goat serum (Invitrogen 10000C) or Mouse on Mouse (M.O.M) blocking reagent (Vector Laboratories, MKB-2213) as appropriate prior to overnight incubation at 4°C with primary antibodies. The following day, slides were incubated with Alexa Fluor conjugated secondary antibodies and mounted using Fluorescence Mounting Medium (Agilent Dako, S302380). Fluorescent images were captured using a Nikon A1 confocal microscope.

**Image Analysis:** Muscle morphology was analyzed on stitched panoramic images of the entire muscle cross-section by high-throughput fully automated image analysis with the MuscleJ plugin for FIJI/ImageJ (Mayeuf-Louchart et al., 2018). Immune cells and satellite cells were manually counted throughout the entire cross-section and then normalized to tissue area as determined by MuscleJ. In all cases, the experimenter was blinded to the experimental group.

**Muscle Force Testing:** At day 14 post-injury maximum in-situ nerve-stimulated isometric tetanic force ( $P_0$ ) generated by the TA muscle was measured and used to calculate maximal specific isometric force ( $sP_0$ ) by dividing  $P_0$  by muscle cross-sectional area (CSA).

451 **Mediator lipidomics:** Muscle homogenates were analyzed by LC-MS/MS based metabolipidomic  
452 profiling following solid phase extraction as previously described (Markworth et al., 2020; Markworth et al.,  
453 2016; Markworth et al., 2013; Vella et al., 2019).

454 **RT-PCR:** Whole muscle gene expression was measured by RT-PCR on a CFX96 Real-Time PCR  
455 Detection System (Bio-Rad, 1855195) in 20  $\mu$ L reactions of iTaq™ Universal SYBR® Green Supermix (Bio-  
456 Rad, #1725124) with 1  $\mu$ M forward and reverse primers (Table 1). Relative mRNA expression was determined  
457 using the  $2^{-\Delta\Delta C_t}$  method. Primers are listed in Table 1.

458 **Flow Cytometry:** Muscle tissue was digested with collagenase II/dispase. Isolated single-cells were Fc  
459 blocked prior to incubation with fluorescently conjugated primary antibodies. Cells were run on a flow  
460 cytometer and data was analyzed with FlowJo 10 software.

461 **Statistics:** Data is presented as the mean  $\pm$  SEM. Statistical analysis was performed in GraphPad Prism  
462 7. Between group differences were tested by two-tailed unpaired students t-tests (2 groups) or by a one-way  
463 analysis of variance (ANOVA) followed by pair-wise Least Significance Difference (LSD) (3 groups) or Holm-  
464 Sidak post-hoc tests ( $>3$  groups).  $p \leq 0.05$  was used to determine statistical significance.

465 **Study approval:** All animal experiments were approved by the University of Michigan Institutional  
466 Animal Care and Use committee (IACUC) (PRO00008744).

#### 467 **Acknowledgments:**

468 This work was supported by the Glenn Foundation for Medical Research Post-Doctoral Fellowship in  
469 Aging Research (JFM), the National Institutes of Health (NIH) under the awards R01 (AG050676) (SVB), PO1  
470 (AG051442) (SVB), P30 (AR069620) (CAA, SVB) and S10 (RR027926) (KRM), together with the 3M  
471 Foundation (CAA), American Federation for Aging Research (CAA), the University of Michigan Geriatrics  
472 Center/National Institute of Aging P30 (AG024824) (CAA, SVB), the University of Michigan Biomedical  
473 Engineering Department (CAA), and the Department of Defense and Congressionally Directed Medical  
474 Research Program W81XWH18SBAA1-1257992 (CAA).

#### 475 **Conflict of Interest Statement:**

476 The authors declare no conflicts of interest.

#### 478 **Author contributions:**

479 J.F.M and S.V.B conceived the study. S.V.B, K.R.M, P.C.D.M and C.A.A supervised the work. J.F.M,  
480 L.A.B, C.A.A, and S.V.B designed the experiments. J.F.M, L.A.B, E.L, J.L, J.A.C-M, and C.D performed the  
This article is protected by copyright. All rights reserved



481 experiments. J.F.M, L.A.B, J.L, and K.R.M analyzed the data. J.F.M prepared the figures and wrote the  
482 manuscript with input from all authors.

483 **Data Availability Statement:**

484 Original data will be made available upon request.

Author Manuscript

505 **References:**

- 506 Arita, M., Bianchini, F., Aliberti, J., Sher, A., Chiang, N., Hong, S., . . . Serhan, C. N. (2005). Stereochemical  
507 assignment, antiinflammatory properties, and receptor for the omega-3 lipid mediator resolvin E1. *J Exp*  
508 *Med*, *201*(5), 713-722. doi:10.1084/jem.20042031
- 509 Arnardottir, H. H., Dalli, J., Colas, R. A., Shinohara, M., & Serhan, C. N. (2014). Aging delays resolution of  
510 acute inflammation in mice: reprogramming the host response with novel nano-proresolving medicines.  
511 *J Immunol*, *193*(8), 4235-4244. doi:10.4049/jimmunol.1401313
- 512 Arnold, L., Henry, A., Poron, F., Baba-Amer, Y., van Rooijen, N., Plonquet, A., . . . Chazaud, B. (2007).  
513 Inflammatory monocytes recruited after skeletal muscle injury switch into antiinflammatory  
514 macrophages to support myogenesis. *J Exp Med*, *204*(5), 1057-1069. doi:10.1084/jem.20070075
- 515 Blanc, R. S., Kallenbach, J. G., Bachman, J. F., Mitchell, A., Paris, N. D., & Chakkalakal, J. V. (2020).  
516 Inhibition of inflammatory CCR2 signaling promotes aged muscle regeneration and strength recovery  
517 after injury. *Nat Commun*, *11*(1), 4167. doi:10.1038/s41467-020-17620-8
- 518 Blau, H. M., Cosgrove, B. D., & Ho, A. T. (2015). The central role of muscle stem cells in regenerative failure  
519 with aging. *Nat Med*, *21*(8), 854-862. doi:10.1038/nm.3918
- 520 Chiang, N., & Serhan, C. N. (2020). Specialized pro-resolving mediator network: an update on production and  
521 actions. *Essays Biochem*, *64*(3), 443-462. doi:10.1042/EBC20200018
- 522 Christmas, P. (2015). Role of Cytochrome P450s in Inflammation. *Adv Pharmacol*, *74*, 163-192.  
523 doi:10.1016/bs.apha.2015.03.005
- 524 Cui, C. Y., Driscoll, R. K., Piao, Y., Chia, C. W., Gorospe, M., & Ferrucci, L. (2019). Skewed macrophage  
525 polarization in aging skeletal muscle. *Aging Cell*, *18*(6), e13032. doi:10.1111/accel.13032
- 526 Faulkner, J. A., Larkin, L. M., Claflin, D. R., & Brooks, S. V. (2007). Age-related changes in the structure and  
527 function of skeletal muscles. *Clin Exp Pharmacol Physiol*, *34*(11), 1091-1096. doi:10.1111/j.1440-  
528 1681.2007.04752.x
- 529 Gangemi, S., Lucioti, G., D'Urbano, E., Mallamace, A., Santoro, D., Bellinghieri, G., . . . Romano, M. (2003).  
530 Physical exercise increases urinary excretion of lipoxin A4 and related compounds. *J Appl Physiol*  
531 *(1985)*, *94*(6), 2237-2240. doi:10.1152/jappphysiol.01004.2002
- 532 Giannakis, N., Sansbury, B. E., Patsalos, A., Hays, T. T., Riley, C. O., Han, X., . . . Nagy, L. (2019). Dynamic  
533 changes to lipid mediators support transitions among macrophage subtypes during muscle regeneration.  
534 *Nat Immunol*, *20*(5), 626-636. doi:10.1038/s41590-019-0356-7
- 535 Gilroy, D. W., Edin, M. L., De Maeyer, R. P., Bystrom, J., Newson, J., Lih, F. B., . . . Bishop-Bailey, D. (2016).  
536 CYP450-derived oxylipins mediate inflammatory resolution. *Proc Natl Acad Sci U S A*, *113*(23), E3240-  
537 3249. doi:10.1073/pnas.1521453113

- 538 Halade, G. V., Kain, V., Black, L. M., Prabhu, S. D., & Ingle, K. A. (2016). Aging dysregulates D- and E-series  
539 resolvins to modulate cardiopulmonary and cardiorenal network following myocardial infarction. *Aging*  
540 (*Albany NY*), 8(11), 2611-2634. doi:10.18632/aging.101077
- 541 Hiram, R., Xiong, F., Naud, P., Xiao, J., Sirois, M., Tanguay, J. F., . . . Nattel, S. (2020). The inflammation-  
542 resolution promoting molecule resolvin-D1 prevents atrial proarrhythmic remodeling in experimental  
543 right heart disease. *Cardiovasc Res*. doi:10.1093/cvr/cvaa186
- 544 Hong, S., Gronert, K., Devchand, P. R., Moussignac, R. L., & Serhan, C. N. (2003). Novel docosatrienes and  
545 17S-resolvins generated from docosahexaenoic acid in murine brain, human blood, and glial cells.  
546 Autacoids in anti-inflammation. *J Biol Chem*, 278(17), 14677-14687. doi:10.1074/jbc.M300218200
- 547 Jensen, S. M., Bechshoff, C. J. L., Heisterberg, M. F., Schjerling, P., Andersen, J. L., Kjaer, M., & Mackey, A.  
548 L. (2020). Macrophage Subpopulations and the Acute Inflammatory Response of Elderly Human  
549 Skeletal Muscle to Physiological Resistance Exercise. *Front Physiol*, 11, 811.  
550 doi:10.3389/fphys.2020.00811
- 551 Kawanishi, N., & Machida, S. (2021). Alterations of macrophage and neutrophil content in skeletal muscle of  
552 aged versus young mice. *Muscle Nerve*. doi:10.1002/mus.27158
- 553 Krashia, P., Cordella, A., Nobili, A., La Barbera, L., Federici, M., Leuti, A., . . . Mercuri, N. B. (2019). Blunting  
554 neuroinflammation with resolvin D1 prevents early pathology in a rat model of Parkinson's disease. *Nat*  
555 *Commun*, 10(1), 3945. doi:10.1038/s41467-019-11928-w
- 556 Li, J., Yi, X., Yao, Z., Chakkalakal, J. V., Xing, L., & Boyce, B. F. (2020). TNF Receptor-Associated Factor 6  
557 Mediates TNF $\alpha$ -Induced Skeletal Muscle Atrophy in Mice During Aging. *J Bone Miner Res*, 35(8),  
558 1535-1548. doi:10.1002/jbmr.4021
- 559 Lockhart, N. C., & Brooks, S. V. (2008). Neutrophil accumulation following passive stretches contributes to  
560 adaptations that reduce contraction-induced skeletal muscle injury in mice. *J Appl Physiol (1985)*,  
561 104(4), 1109-1115. doi:10.1152/jappphysiol.00850.2007
- 562 Markworth, J. F., Brown, L. A., Lim, E., Floyd, C., Larouche, J., Castor-Macias, J. A., . . . Brooks, S. V. (2020).  
563 Resolvin D1 supports skeletal myofiber regeneration via actions on myeloid and muscle stem cells. *JCI*  
564 *Insight*, 5(18). doi:10.1172/jci.insight.137713
- 565 Markworth, J. F., Maddipati, K. R., & Cameron-Smith, D. (2016). Emerging roles of pro-resolving lipid  
566 mediators in immunological and adaptive responses to exercise-induced muscle injury. *Exerc Immunol*  
567 *Rev*, 22, 110-134.
- 568 Markworth, J. F., Vella, L., Lingard, B. S., Tull, D. L., Rupasinghe, T. W., Sinclair, A. J., . . . Cameron-Smith,  
569 D. (2013). Human inflammatory and resolving lipid mediator responses to resistance exercise and

- 570 ibuprofen treatment. *Am J Physiol Regul Integr Comp Physiol*, 305(11), R1281-1296.  
571 doi:10.1152/ajpregu.00128.2013
- 572 Mayeuf-Louchart, A., Hardy, D., Thorel, Q., Roux, P., Gueniot, L., Briand, D., . . . Danckaert, A. (2018).  
573 MuscleJ: a high-content analysis method to study skeletal muscle with a new Fiji tool. *Skelet Muscle*,  
574 8(1), 25. doi:10.1186/s13395-018-0171-0
- 575 McArthur, S., Juban, G., Gobbetti, T., Desgeorges, T., Theret, M., Gondin, J., . . . Mounier, R. (2020). Annexin  
576 A1 drives macrophage skewing to accelerate muscle regeneration through AMPK activation. *J Clin*  
577 *Invest*, 130(3), 1156-1167. doi:10.1172/JCI124635
- 578 Mukherjee, P. K., Marcheselli, V. L., Serhan, C. N., & Bazan, N. G. (2004). Neuroprotectin D1: a  
579 docosahexaenoic acid-derived docosatriene protects human retinal pigment epithelial cells from  
580 oxidative stress. *Proc Natl Acad Sci U S A*, 101(22), 8491-8496. doi:10.1073/pnas.0402531101
- 581 Patsalos, A., Simandi, Z., Hays, T. T., Peloquin, M., Hajian, M., Restrepo, I., . . . Nagy, L. (2018). In vivo  
582 GDF3 administration abrogates aging related muscle regeneration delay following acute sterile injury.  
583 *Aging Cell*, 17(5), e12815. doi:10.1111/accel.12815
- 584 Rahman, F. A., Angus, S. A., Stokes, K., Karpowicz, P., & Krause, M. P. (2020). Impaired ECM Remodeling  
585 and Macrophage Activity Define Necrosis and Regeneration Following Damage in Aged Skeletal  
586 Muscle. *Int J Mol Sci*, 21(13). doi:10.3390/ijms21134575
- 587 Reidy, P. T., McKenzie, A. I., Mahmassani, Z. S., Petrocelli, J. J., Nelson, D. B., Lindsay, C. C., . . .  
588 Drummond, M. J. (2019). Aging impairs mouse skeletal muscle macrophage polarization and muscle-  
589 specific abundance during recovery from disuse. *Am J Physiol Endocrinol Metab*, 317(1), E85-E98.  
590 doi:10.1152/ajpendo.00422.2018
- 591 Rymut, N., Heinz, J., Sadhu, S., Hosseini, Z., Riley, C. O., Marinello, M., . . . Fredman, G. (2020). Resolvin D1  
592 promotes efferocytosis in aging by limiting senescent cell-induced MerTK cleavage. *FASEB J*, 34(1),  
593 597-609. doi:10.1096/fj.201902126R
- 594 Sansbury, B. E., Li, X., Wong, B., Patsalos, A., Giannakis, N., Zhang, M. J., . . . Spite, M. (2020). Myeloid  
595 ALX/FPR2 regulates vascularization following tissue injury. *Proc Natl Acad Sci U S A*, 117(25), 14354-  
596 14364. doi:10.1073/pnas.1918163117
- 597 Schwab, J. M., Chiang, N., Arita, M., & Serhan, C. N. (2007). Resolvin E1 and protectin D1 activate  
598 inflammation-resolution programmes. *Nature*, 447(7146), 869-874. doi:10.1038/nature05877
- 599 Serhan, C. N., Hamberg, M., & Samuelsson, B. (1984). Lipoxins: novel series of biologically active compounds  
600 formed from arachidonic acid in human leukocytes. *Proc Natl Acad Sci U S A*, 81(17), 5335-5339.  
601 doi:10.1073/pnas.81.17.5335

- 602 Serhan, C. N., Hong, S., Gronert, K., Colgan, S. P., Devchand, P. R., Mirick, G., & Moussignac, R. L. (2002).  
603 Resolvins: a family of bioactive products of omega-3 fatty acid transformation circuits initiated by  
604 aspirin treatment that counter proinflammation signals. *J Exp Med*, *196*(8), 1025-1037.  
605 doi:10.1084/jem.20020760
- 606 Serhan, C. N., Yang, R., Martinod, K., Kasuga, K., Pillai, P. S., Porter, T. F., . . . Spite, M. (2009). Maresins:  
607 novel macrophage mediators with potent antiinflammatory and proresolving actions. *J Exp Med*, *206*(1),  
608 15-23. doi:10.1084/jem.20081880
- 609 Sloboda, D. D., Brown, L. A., & Brooks, S. V. (2018). Myeloid Cell Responses to Contraction-induced Injury  
610 Differ in Muscles of Young and Old Mice. *J Gerontol A Biol Sci Med Sci*, *73*(12), 1581-1590.  
611 doi:10.1093/gerona/gly086
- 612 Sorensen, J. R., Kaluhiokalani, J. P., Hafen, P. S., Deyhle, M. R., Parcell, A. C., & Hyldahl, R. D. (2019). An  
613 altered response in macrophage phenotype following damage in aged human skeletal muscle:  
614 implications for skeletal muscle repair. *FASEB J*, *33*(9), 10353-10368. doi:10.1096/fj.201900519R
- 615 Sun, Y. P., Oh, S. F., Uddin, J., Yang, R., Gotlinger, K., Campbell, E., . . . Serhan, C. N. (2007). Resolvin D1  
616 and its aspirin-triggered 17R epimer. Stereochemical assignments, anti-inflammatory properties, and  
617 enzymatic inactivation. *J Biol Chem*, *282*(13), 9323-9334. doi:10.1074/jbc.M609212200
- 618 Tidball, J. G., Flores, I., Welc, S. S., Wehling-Henricks, M., & Ochi, E. (2021). Aging of the immune system  
619 and impaired muscle regeneration: A failure of immunomodulation of adult myogenesis. *Exp Gerontol*,  
620 *145*, 111200. doi:10.1016/j.exger.2020.111200
- 621 Tourki, B., Kain, V., Pullen, A. B., Norris, P. C., Patel, N., Arora, P., . . . Halade, G. V. (2020). Lack of  
622 resolution sensor drives age-related cardiometabolic and cardiorenal defects and impedes inflammation-  
623 resolution in heart failure. *Mol Metab*, *31*, 138-149. doi:10.1016/j.molmet.2019.10.008
- 624 Vella, L., Markworth, J. F., Farnfield, M. M., Maddipati, K. R., Russell, A. P., & Cameron-Smith, D. (2019).  
625 Intramuscular inflammatory and resolving lipid profile responses to an acute bout of resistance exercise  
626 in men. *Physiol Rep*, *7*(13), e14108. doi:10.14814/phy2.14108
- 627 Wang, Y., Wehling-Henricks, M., Samengo, G., & Tidball, J. G. (2015). Increases of M2a macrophages and  
628 fibrosis in aging muscle are influenced by bone marrow aging and negatively regulated by muscle-  
629 derived nitric oxide. *Aging Cell*, *14*(4), 678-688. doi:10.1111/accel.12350
- 630 Zhang, C., Cheng, N., Qiao, B., Zhang, F., Wu, J., Liu, C., . . . Du, J. (2020). Age-related decline of interferon-  
631 gamma responses in macrophage impairs satellite cell proliferation and regeneration. *J Cachexia*  
632 *Sarcopenia Muscle*, *11*(5), 1291-1305. doi:10.1002/jcsm.12584

- 633 Zhang, M. J., Sansbury, B. E., Hellmann, J., Baker, J. F., Guo, L., Parmer, C. M., . . . Spite, M. (2016). Resolvin  
634 D2 Enhances Postischemic Revascularization While Resolving Inflammation. *Circulation*, *134*(9), 666-  
635 680. doi:10.1161/CIRCULATIONAHA.116.021894
- 636 Zheng, J. J., Pena Calderin, E., Hill, B. G., Bhatnagar, A., & Hellmann, J. (2019). Exercise Promotes Resolution  
637 of Acute Inflammation by Catecholamine-Mediated Stimulation of Resolvin D1 Biosynthesis. *J*  
638 *Immunol*, *203*(11), 3013-3022. doi:10.4049/jimmunol.1900144

Author Manuscript

660  
661  
662 **Figure Legends:**

663 **Figure 1 – Age-associated muscle wasting:** **A:** Body weight, tibialis anterior (TA) muscle mass, and relative  
664 TA mass of uninjured young and aged C57BL/6 mice. **B:** Maximal nerve stimulated *in-situ* isometric force ( $P_o$ ,  
665 mN) generated by young and aged TA muscles were measured and used to calculate maximal specific force  
666 ( $sP_o$ , mN/mm<sup>2</sup>). **C:** TA cross-sections were stained with antibodies for type I, IIa, and IIb myosin heavy chain.  
667 Type IIx fibers remain unstained (black). The extracellular matrix was labeled with wheat germ agglutinin  
668 (WGA). Scale bars are 1000  $\mu$ m. Right panels show representative fields of view from deep and superficial  
669 regions of the TA. Scale bars are 200  $\mu$ m. The total number and cross-sectional area (CSA) of each myofiber  
670 and its corresponding fiber type was determined using MuscleJ software. **D:** Quantification of total myofiber  
671 number, mean fiber CSA, and fiber size frequency distribution. **E:** Fiber type composition and mean fiber CSA  
672 split by fiber type. Bars show the mean  $\pm$  SEM of 5-7 mice per group with dots representing data from each  
673 individual mouse. \*Denotes  $p < 0.05$  vs. young mice by two-tailed unpaired t-test.

674  
675  
676  
677  
678  
679  
680  
681  
682  
683  
684  
685  
686  
687

688  
689  
690 **Figure 2 – Chronic inflammation of aged muscle is associated with a deficiency of proresolving lipid**  
691 **mediators: A-B:** Principle component analysis (PCA) score and loading plots of the mediator lipidome of  
692 uninjured TA muscles from young and aged C57BL/6 mice as determined by liquid chromatography-tandem  
693 mass spectrometry (LC-MS/MS). **C:** Volcano plots summarizing the magnitude and statistical significance of  
694 difference between aged and young mice for each individual detected lipid mediator. Complete volcano plot  
695 data is shown in Supplemental Table 2. **D:** Relative pooled concentrations (pmol/mg tissue) of lipid mediator  
696 metabolites of ARA, EPA, and DHA derived from major enzymatic biosynthesis pathway in young and aged  
697 mice. Linoleic acid metabolites (e.g. HODES and EpOMEs) are excluded and shown separately in  
698 Supplemental Table 1. **E-F:** TA mRNA expression of inflammation-related genes as determined by real-time  
699 quantitative reverse transcription PCR (RT-qPCR). **H-L:** Quantification of intramuscular number of neutrophils  
700 (Ly6G<sup>+</sup> cells), total macrophages (MΦ) (CD68<sup>+</sup> cells), M2-like MΦ (CD68<sup>+</sup>CD163<sup>+</sup> cells), M1-like MΦ  
701 (CD68<sup>+</sup>CD163<sup>-</sup> cells), and centrally nucleated (regenerating) myofibers. **M:** Representative staining of cross-  
702 sections of young and aged TA muscles. Scale bars are 100 μm for neutrophils and 200 μm for MΦ. Bars show  
703 the mean ± SEM of 5-7 mice per group with dots representing data from each individual mouse. \*Denotes  
704 p<0.05 vs vehicle group by two-tailed unpaired t-test.

705  
706  
707  
708  
709  
710  
711  
712  
713  
714  
715  
716



717  
718  
719 **Figure 3 – Impact of age on local shifts in lipid mediator biosynthesis following muscle injury:** **A:** Young  
720 and aged C57BL/6 mice received bilateral intramuscular injection of the TA muscle with 50  $\mu$ L of 1.2% barium  
721 chloride ( $\text{BaCl}_2$ ) to induce myofiber injury. TA muscles were collected at 1, 3, and 5 days' post-injury for  
722 analysis of intramuscular lipid mediator concentrations via LC-MS/MS. PCA score and loading plots show  
723 global shifts in the mediator lipidome of injured muscle. **B:** Changes in pooled lipid mediator metabolites of  
724 ARA, EPA, and DHA from potential biosynthetic routes. Data is presented as the change in concentration  
725 (pmol/mg tissue) from age-matched uninjured muscles displayed in Figure 2D. Linoleic acid metabolites (e.g.  
726 HODES and EpOMEs) are excluded and shown separately in Supplemental Table 1. **C:** Heat map summarizing  
727 average temporal shifts in representative individual lipid mediators. Statistical analysis of these analytes by two-  
728 way ANOVA is shown in Supplemental Figure 2. **D:** Shifts in the balance of major eicosanoids ( $\text{TXB}_2$ ,  $\text{PGD}_2$ ,  
729  $\text{PGE}_2$ ,  $\text{PGF}_{2\alpha}$ ,  $6\text{kPGF}_{1\alpha}$ , and 5-, 12-, 15-HETEs) relative to detected proresolving mediators ( $\text{RvE3}$ , 8-oxo $\text{RvD1}$ ,  
730  $\text{LXA}_4$ ,  $\text{RvD6}$ ,  $\text{PD1}$ ,  $\text{PDX}$ , and  $\text{MaR1}$ ) and related pathway markers (5-, 18-HEPEs and 4-, 7-, 14, 17- HDoHEs)  
731 following muscle injury. **E:** Changes in the mass of muscle samples used for lipidomic profiling. **F:** Volcano  
732 plots summarizing the magnitude and statistical significance of difference between aged and young mice for  
733 each individual detected lipid mediator. Bars show the mean  $\pm$  SEM of 5-7 mice per group. **B-E:** \*denotes  
734  $p < 0.05$  change from age-matched uninjured muscles as determined by two-way ANOVA with Holm-Sidak  
735 post-hoc tests. #denotes  $p < 0.05$  between young and aged mice at a given time-point by two-way ANOVA with  
736 Holm-Sidak post-hoc tests.

746  
747  
748  
749 **Figure 4 – The effect of aging and RvD1 treatment on the inflammatory response to muscle injury: A-B:**  
750 Young and aged C57BL/6 mice received bilateral intramuscular injection of the TA muscle with 50  $\mu$ L of 1.2%  
751 BaCl<sub>2</sub> to induce myofiber injury. Aged mice were treated daily with RvD1 (100 ng) or vehicle (0.1% ethanol)  
752 via intraperitoneal (IP) injection. TA muscles were collected at day 1 and 3 post-injury and muscle cross-  
753 sections were stained for neutrophils (Ly6G) or monocytes/macrophages (M $\Phi$ , CD68). Cell nuclei and the basal  
754 lamina were counterstained with DAPI and a laminin antibody respectively. Scale bars are 200  $\mu$ m. **C-D:**  
755 Quantification of neutrophils (Ly6G<sup>+</sup> cells) and M $\Phi$  (CD68<sup>+</sup> cells) in injured muscle at day 1 and 3 post-injury.  
756 **E:** Intramuscular neutrophils (Ly6G<sup>+</sup> cells) and M $\Phi$  (CD64<sup>+</sup> cells) as percentage of total intramuscular  
757 leukocytes (CD45<sup>+</sup> cells) as determined by flow cytometry. **F:** Quantification of mRNA expression of muscle  
758 cytokine expression at day 1 post-injury by RT-PCR. Bars show the mean  $\pm$  SEM of 4-7 mice per group with  
759 dots representing data from each individual mouse. \*Denotes p<0.05 between groups by one-way ANOVA with  
760 pairwise LSD post-hoc tests.

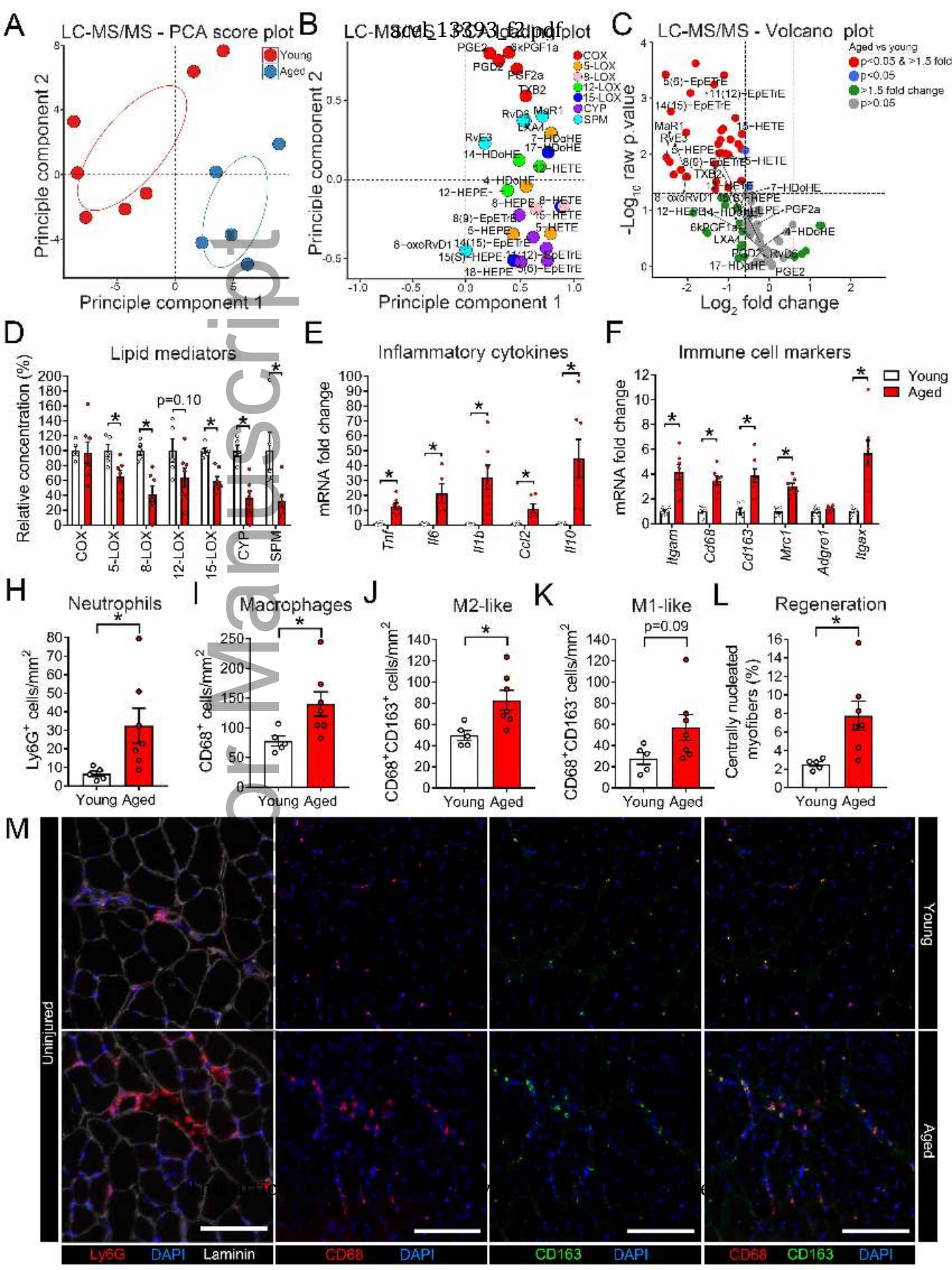
774  
775  
776  
777  
778 **Figure 5 – The effect of age and RvD1 treatment on myofiber regeneration:** **A:** Young and aged C57BL/6  
779 mice received bilateral intramuscular injection of the TA muscle with 50  $\mu$ L of 1.2% BaCl<sub>2</sub> to induce myofiber  
780 injury. Aged mice were treated daily with RvD1 (100 ng) or vehicle (0.1% ethanol) by IP injection. TA muscles  
781 were collected at day 5 post-injury and muscle cross-sections were stained for embryonic myosin heavy chain  
782 (eMHC). Cell nuclei and the basal lamina were counterstained with DAPI and a laminin antibody respectively.  
783 Scale bars are 200  $\mu$ m. **B:** Quantitative of total myofiber number, regenerating (centrally nucleated) myofiber  
784 number, and the percentage of total myofibers undergoing regeneration as determined by MuscleJ. **C:** Mean  
785 CSA of the regenerating myofiber population. **D:** Frequency distribution regenerating myofiber CSA in young  
786 and aged mice. **E:** Muscle cross-sections were stained for total M $\Phi$  (CD68) and M2-like M $\Phi$  (CD163). Scale  
787 bars are 200  $\mu$ m. **F:** Quantification of total M $\Phi$  infiltration as percentage of tissue area containing CD68<sup>+</sup>  
788 staining and M2-like M $\Phi$  (CD163<sup>+</sup> cell) counts. **G:** Muscle cross-sections were stained for the muscle satellite  
789 cell marker Pax7 at day 5 post-injury. TA muscles from age matched uninjured mice served as controls. Scale  
790 bars are 100  $\mu$ m. **H:** Quantification of satellite cell number expressed relative to tissue area or myofiber  
791 number. Bars are mean  $\pm$  SEM of 5-7 mice per group with dots representing data for each individual mouse.  
792 \*p<0.05 by one-way ANOVA with pairwise LSD post-hoc tests for panels A-F or pairwise Holm-Sidak post-  
793 hoc tests for panel H.

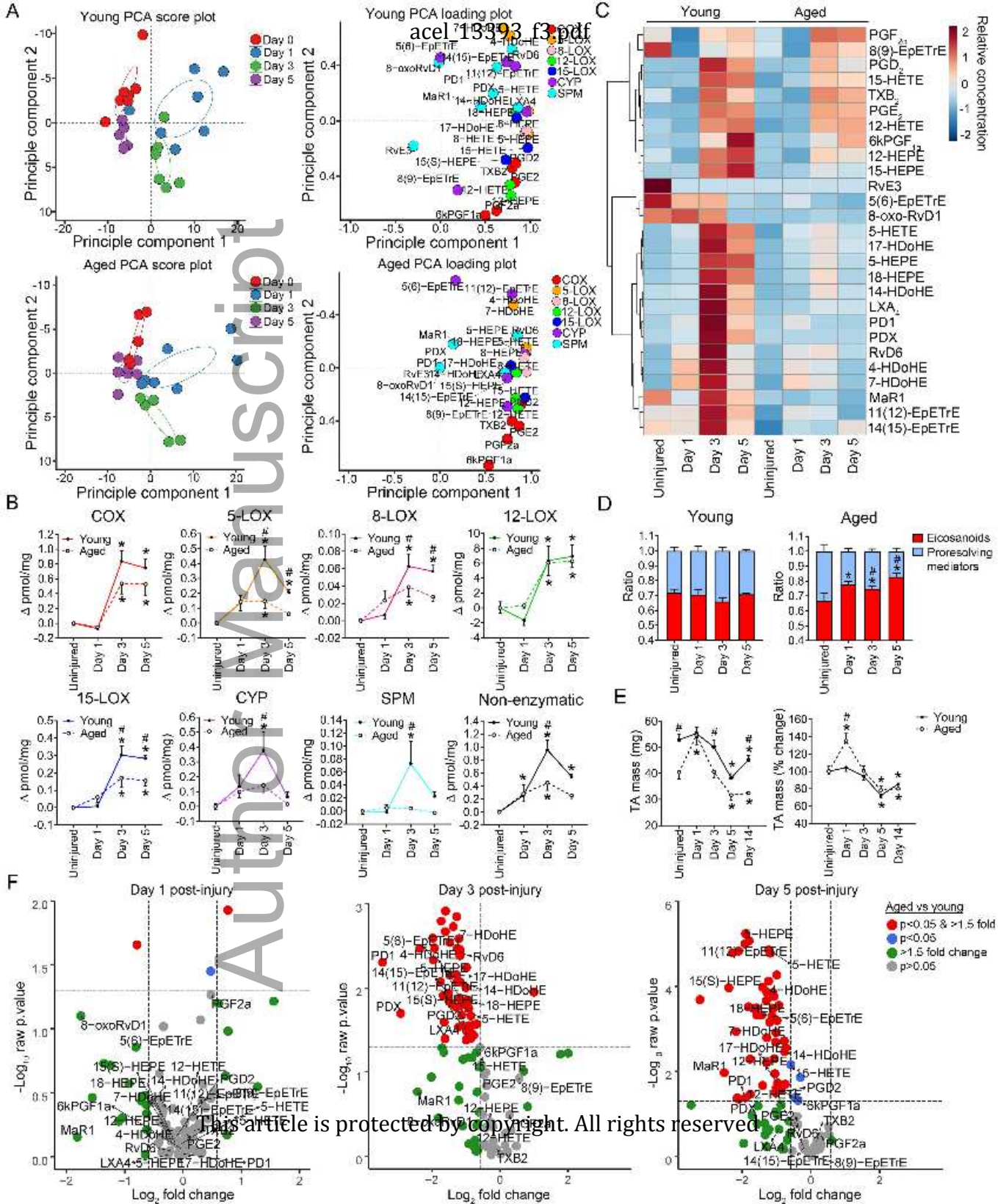
803  
804  
805  
806  
807 **Figure 6 – RvD1 limits maladaptive remodeling following muscle injury in aged mice:** **A:** Young and aged  
808 C57BL/6 mice received bilateral intramuscular injection of the TA muscle with 50  $\mu$ L of 1.2% BaCl<sub>2</sub> to induce  
809 myofiber injury. Aged mice were treated with daily IP injections of RvD1 (100 ng) or vehicle (0.1% ethanol)  
810 for 14 days. On day 14 post-injury maximal nerve-stimulated *in-situ* isometric force ( $P_o$ , mN) generated by the  
811 TA muscle was measured and used to calculate specific force ( $sP_o$ , mN/mm<sup>2</sup>). Data is presented as percentage  
812 force deficit relative to age-matched uninjured TA muscles shown in Figure 1B. **B:** TA cross-sections were  
813 stained for hematoxylin & eosin, conjugated phalloidin (actin), or with antibodies against type I, IIa, and IIb  
814 myosin heavy chain. Type IIx fibers remain unstained (black). Cell nuclei and the basal lamina were  
815 counterstained with DAPI and a laminin antibody on phalloidin slides. The extracellular matrix was stained  
816 with wheat germ agglutinin (WGA) to delineate myofiber boundaries on fiber type slides. Scale bars are 200  
817  $\mu$ m. Image analysis was performed using MuscleJ software. **C:** Whole regenerating muscle CSA and relative  
818 amounts of tissue area containing contractile myofibers (actin<sup>+</sup> area) compared with extracellular matrix (actin<sup>-</sup>  
819 tissue area). **D:** The fiber type composition of regenerating muscles from young and aged mice. **E:**  
820 Quantification of regenerating (centrally nucleated) myofiber number, percentage of total fibers undergoing  
821 regeneration, and the mean CSA/frequency distribution of the centrally nucleated fiber population. Bars show  
822 mean  $\pm$  SEM of 5-10 mice per group with dots representing data from each individual mouse \*Denotes  $p < 0.05$   
823 by one-way ANOVA with pairwise LSD post-hoc tests.

**Table 1:** Real-time PCR primers

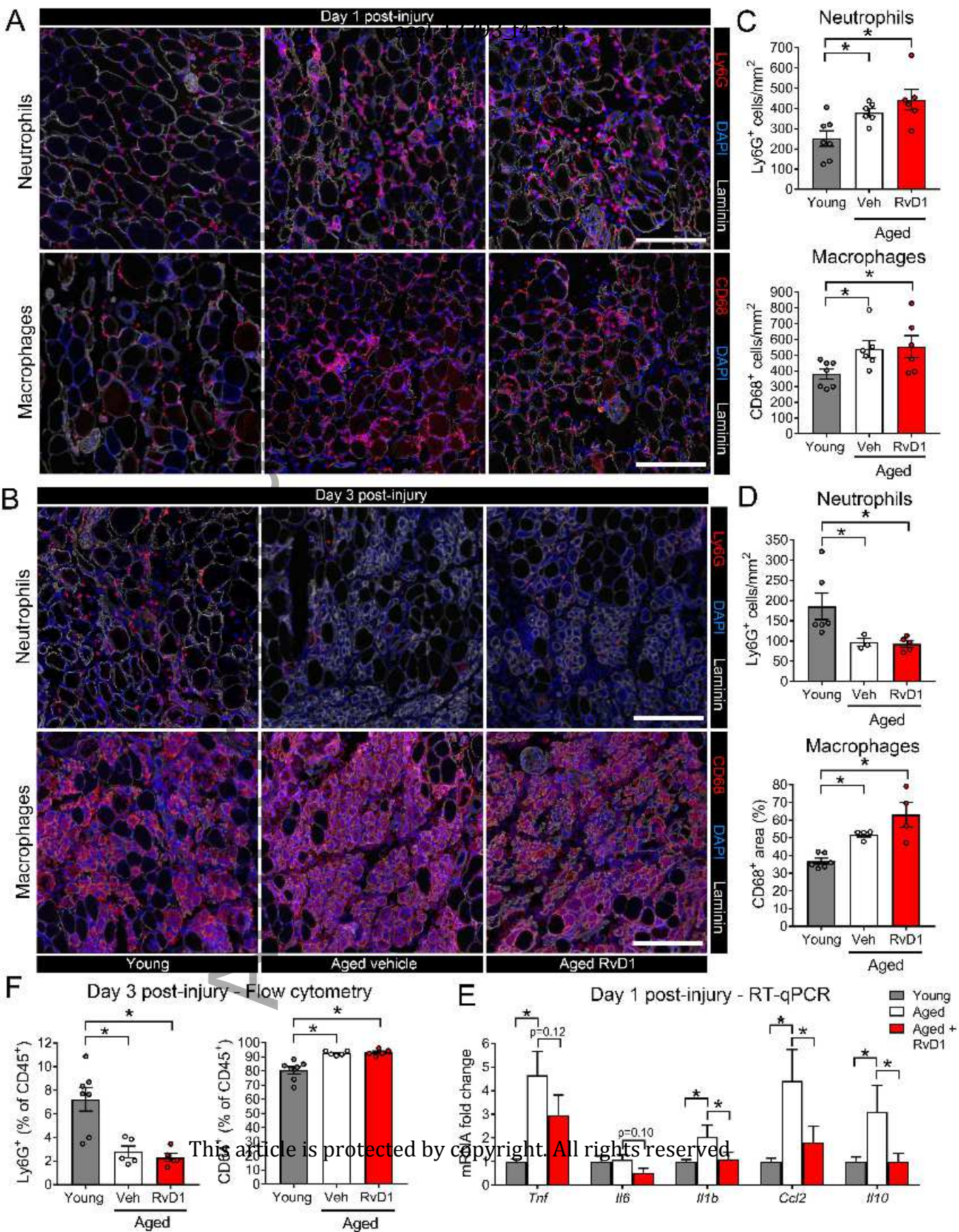
Gene	Primer	Sequence
<i>Tnf1</i>	Forward	ATGGCCTCCCTCTCATCAGT
	Reverse	TGGTTTGCTACGACGTGGG
<i>Il6</i>	Forward	TCCGGAGAGGAGACTTCACA
	Reverse	TTGCCATTGCACAACTCTTTTCT
<i>Il1b</i>	Forward	GCCACCTTTTGACAGTGATGAG
	Reverse	GACAGCCCAGGTCAAAGGTT
<i>Ccl2</i>	Forward	AGCTGTAGTTTTTGTCAACAAGC
	Reverse	GACCTTAGGGCAGATGCAGT
<i>Il10</i>	Forward	GGCGCTGTCATCGATTTCTC
	Reverse	ATGGCCTTGTAGACACCTTGG
<i>Itgam</i>	Forward	TGGCCTATAACAAGCTTGGCTTT
	Reverse	AAAGGCCGTTACTGAGGTGG
<i>Cd68</i>	Forward	ACTGGTGTAGCCTAGCTGGT
	Reverse	CCTTGGGCTATAAGCGGTCC
<i>Cd163</i>	Forward	TCTCCTGGTTGTAAAAGGTTTGT
	Reverse	CAGTTGTTTTACCACCCGC
<i>Mrc1</i>	Forward	GGCTGATTACGAGCAGTGGA
	Reverse	CATCACTCCAGGTGAACCCC
<i>Adgre1</i>	Forward	CCAGGAGTGGAAATGTCAAGATGT
	Reverse	GCAGACTGAGTTAGGACCACA
<i>Itgax</i>	Forward	GCAGACACTGAGTGATGCCA
	Reverse	TCGGAGGTCACCTAGTTGGG
<i>Actb</i>	Forward	CACTGTCGAGTCGCGTCC

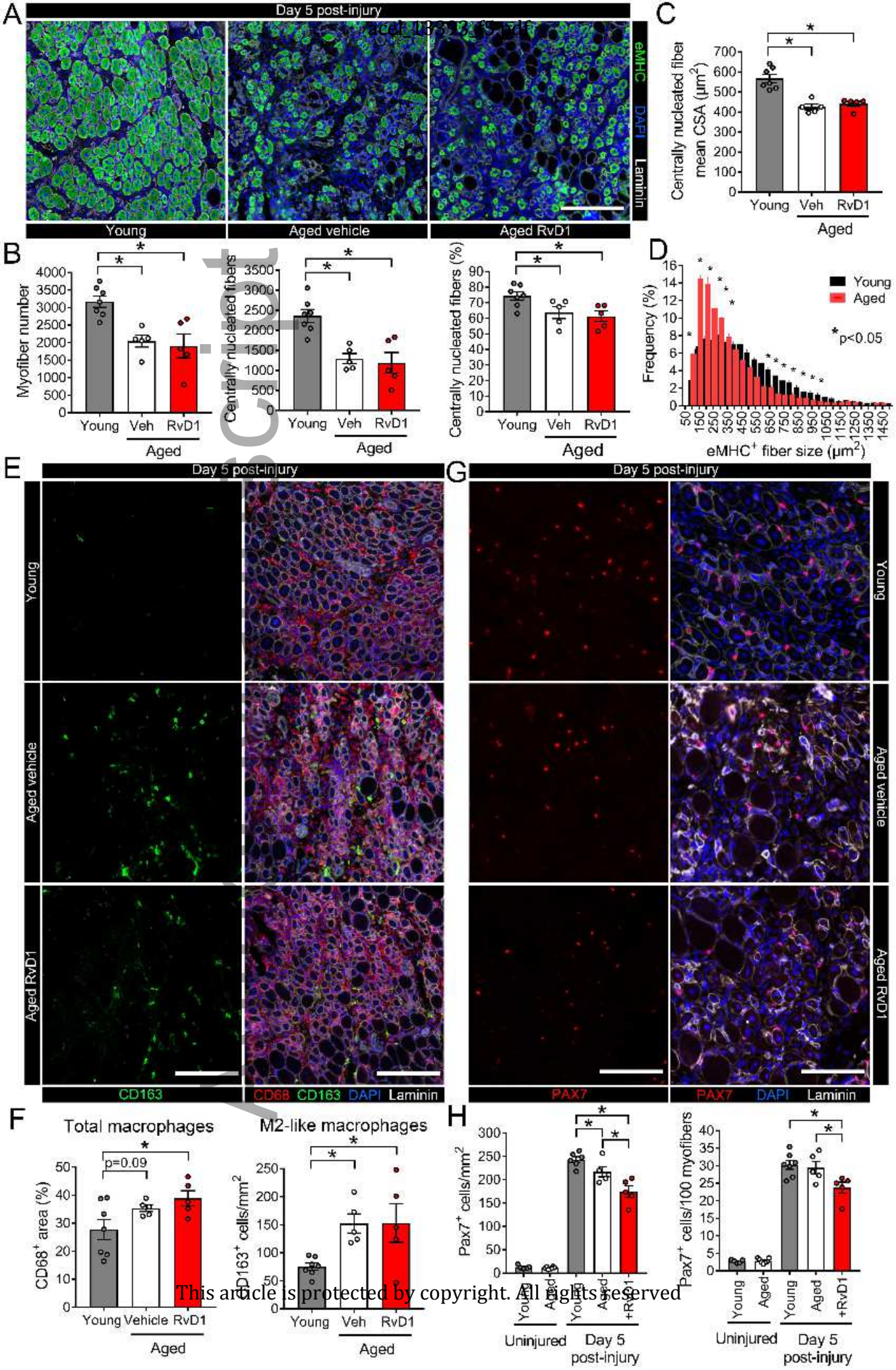


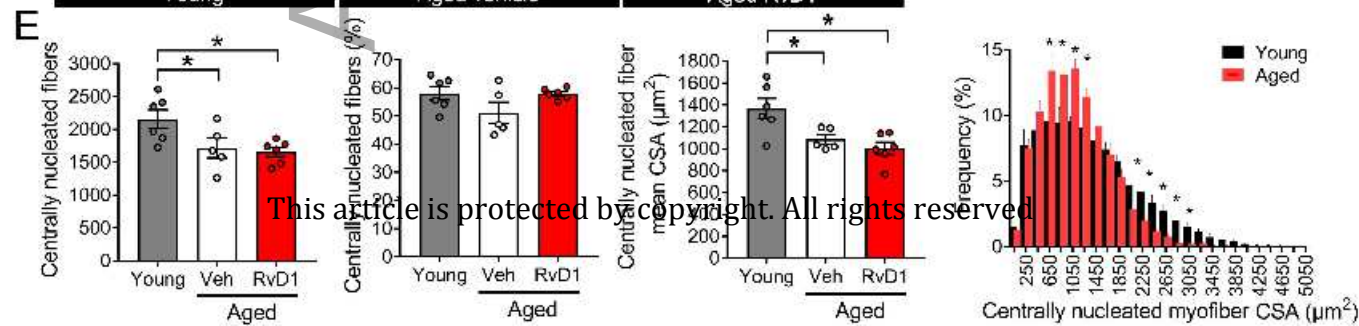
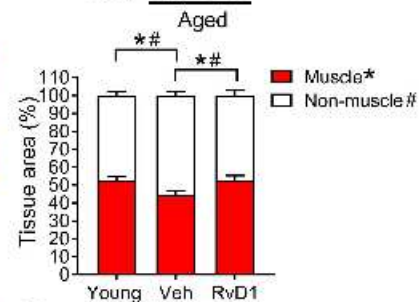
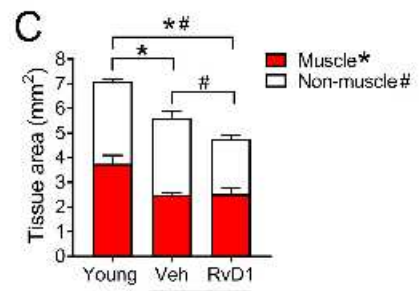
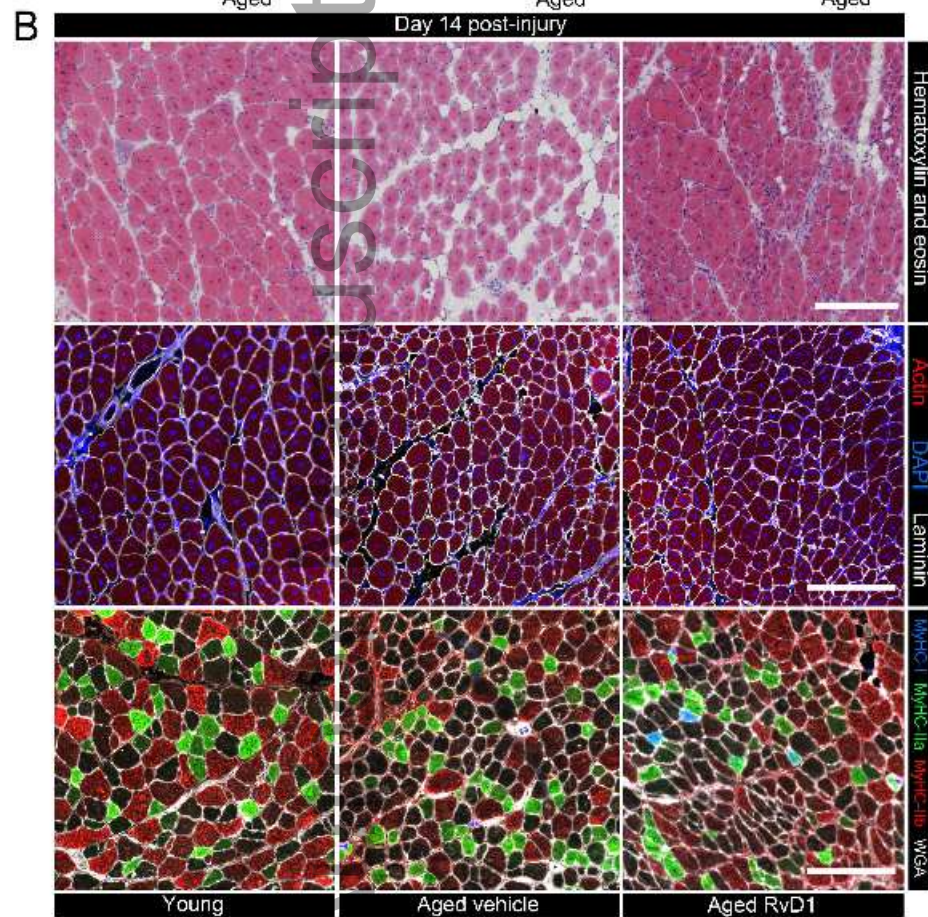
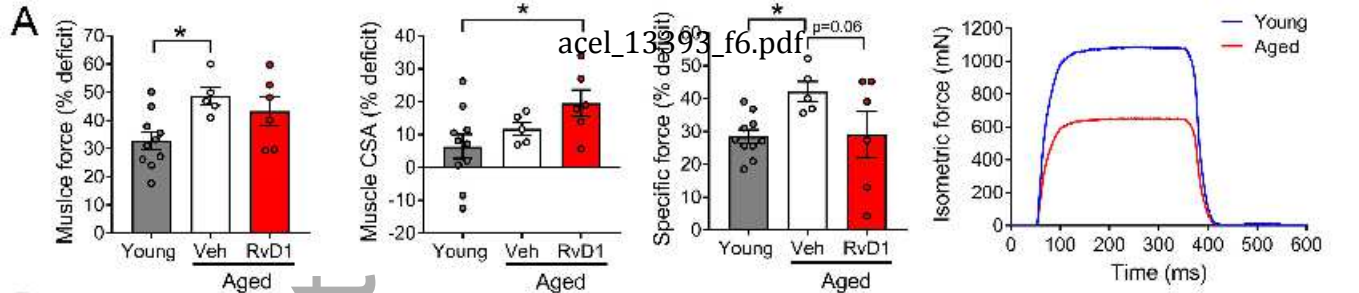












This article is protected by copyright. All rights reserved